MONITORING OF LAND SURFACE TEMPERATURES BASED ON SEVIRI/METEOSAT-9 MEASUREMENTS

Sergey Uspensky, Valery Solovjiev, Alexander Uspensky

SRC Planeta, B.Predtechensky, 7, 123242 Moscow, Russia

ABSTRACT

This paper describes the new methodology developed for operational retrieving of land surface skin temperature (LST or T_s) and emissivity (LSE or E) from SEVIRI/Meteosat-9 data. The clear sky IR brightness temperatures measured at three different times (image cycles) in the SEVIRI split-window (SW) channels N9 (IR 10.8) and N10 (IR 12.0) are converted to the LSTs and LSEs estimates using well-known "local" SW techniques in combination with the two-temperature method. The LSEs are specified as channel 9 and 10 emissivities E_9 and E_{10}. The developed approach employs the hypothesis that E_9 and E_{10} remain constant during the time interval between the first and the last image cycles used; moreover, accurate E_9 and E_{10} first guesses are not required.

The performance of proposed retrieval methodology has been evaluated in the experiments with synthetic and actual SEVIRI/ Meteosat-9 data covering different areas in Europe (with varying zenith angles) for two time periods-in September 2008 and in May-September 2009. For each date three SEVIRI imaging cycles have been used – at 11.00, 12.00, and 13.00 UTC. The cross-validation of LST retrievals has been performed through comparison to independent (synchronous and collocated) SEVIRI-based LST estimates produced at LSA SAF. The results show the RMS deviations in the range 0.9-2.6K.

INTRODUCTION

Land surface temperature (LST or Ts) is an important geophysical parameter and its knowledge at a variety of spatial and temporal scales is of considerable interest for many applications, such as hydrology, agrometeorology, and climate studies. Together with the land surface spectral emissivity or LSE the LST affect the heat and water transport between the surface and the atmosphere. There is a strong need in the remote sensing of Ts, since the conventional surface temperature observations are rather sparse (in space and time).The development of a method for LST derivation based on geostationary satellite data would allow to add some supplementary information to in-situ measurements, or, in some cases, to replace these measurements for a large regions.

In addition, this work was stimulated by the fact that in the nearest future the new Russian geostationary satellite ELECTRO-L with scanner-imager MSU-GS on board is planned to be launched. This sensor has 10 channels, moreover it has 2 IR SW channels similar to SEVIRI/METEOSAT-9 ch. N9 and N10 [7]. It should allow to adjust the proposed approach to MSU-GS data for LST derivation.

The possibilities of extracting LST and SSE information from thermal IR multichannel measurements in the spectral window range has been the subject of numerous investigations during last 20 years, see [1,2]. It seems useful to remind briefly the main problems and disturbing factors which make it difficult to derive an accurate LST information from satellite measurements:

- The spatial and temporal variability of the LSE as well as the fact that it is not precisely known for some types of surfaces [8];
- It is necessary to derive n+1 unknowns {Ts, E_1,…, E_n} from n equations, so the inverse problem of Ts estimation is undetermined. That is why we need an additional information about LSE;

- Spatial (inside one pixel) and time (diurnal cycle, overheating effects) variability of LST causes problems in comparison between satellite and in-situ measurements;
- There could be a big difference in between Ts (LST) and Ta (air temperature at 2 meters height) that impedes the validation of LSTs through comparison with conventional Ta measurements.

The next section contains brief method description. The LST estimates validation performed through comparison with similar LST estimates produced at LSA SAF (Lisbon, Portugal) [5] is discussed in the last section.

METHOD DESCRIPTION

The proposed technique is based on the combination of well-known "local" SWM in combination with the TTM. The clear sky IR brightness temperatures measured at three different times t_1, t_2, t_3 (image cycles) in the SEVIRI split-window channels N9 (IR 10.8) and N10 (IR 12.0) are used for simultaneous derivation of LST and SSE. The developed approach employs the hypothesis that E_9 and E_{10} (further marked as e_1 and e_2) remain constant during the time interval between the first and the last image cycles used: $e_i(t_1)=e_i(t_2)=e_i(t_3)$, i =1, 2.

1. The "local" SWM algorithm can be written as follows [5, 10]:
$T_s = a_1 + (a_2 + a_3\, g_1(e) + a_4\, g_2(e))\,(T_1 + T_2) + (a_5 + a_6\, g_1(e) + a_7\, g_2(e))\,(T_1 - T_2)$,
where T_1 and T_2 are brightness temperatures in IR channels 10.8 and 12.0 accordingly;
$g_2(e) = \Delta e/e^2$, $e = 0.5(e_1 + e_2)$, $\Delta e = e_1 - e_2$; $a_1 - a_7$ are regression coefficients depending on zenith angle θ.

The RTTOV-7 code [6] has been implemented to generate the sample of synthetic SEVIRI measurements in SW channels according to formula:

$$I_j^p(\theta; t_i) = e_j B_j(T_s(t_i))\tau_{js}(\theta; t_i) + I_j^{\uparrow}(\theta; t_i) + (1-e_j)\,\tau_{js}(\theta; t_i)\, I_j^{\downarrow}(\theta; t_i), \quad i = 1, 2, 3;\ j = 1, 2$$

In this equation $I_j^p(\theta; t_i)$ is synthetic radiance in ch.9 (j = 1) and ch.10 (j = 2) at the top of the atmosphere and at the time t_i; $B_j(T_s(t_i))$ is Planck radiance for temperature $T_s(t_i)$ in ch. 9,10; τ_{js} is the total transmittance of the atmosphere for appropriate channels; $I_j^{\uparrow}(\theta; t_i)$, $I_j^{\downarrow}(\theta; t_i)$ are upwelling and downwelling (at the ground level) atmospheric radiances in ch. 9,10, for the angle θ at time t_i.

The regression coefficients $a_i(\theta)$ were determined using the least square fit method for a variety of zenith angles between 0^0 and 55^0 stepping 5^0 and for representative sample of various atmospheric states.

2. The TTM method [3] was used to adjust the measured signals $I_j(\theta; t_i)$ to the synthetic ones $I_j^p(\theta; t_i)$ in the SW channels with help of least-square method.
The minimization of the following function in the TTM method was used to fit the synthetic and measured signals:

$$\Phi_\kappa(T_s(t_1)), T_s(t_2), T_s(t_3), e_1, e_2) = \frac{1}{6}\sum_{i=1}^{3}\sum_{j=1}^{2} [I_j(t_i) - I_j^p(t_i)]^2 \ .$$

3. The method does not require the accurate knowledge of e_1, e_2. It consists of T_s estimation and then an iterative definition of e_1, e_2. The initial reference values for e_1, e_2 (the same for the whole region of interest or ROI) are chosen from the range of 0.95-0.98.

4. The 1^{st} and 2^{nd} steps of the process are repeated iterationally; moreover at each iteration the bias-correction procedure is applied (for detail see [9]).

RESULTS AND CROSS-VALIDATION

The retrievals of T_S were performed only for the clear-sky conditions. In order to get the cloud mask it was used the well known software package MAIA, adopted to SEVIRI data [4].

At the first stage of studies (including experiments with synthetic SEVIRI data and cross-validation with LST products provided by LSA SAF) we investigated the feasibility of T_S estimates for different zenith angles. Two Regions of Interest (ROI) were selected: one with zenith angle 35° - 45° and other with angles 45° - 50°. The comparison with synchronous and collocated LST products from LSA SAF has shown that zenith angle does not strongly affect the discrepancy between the data sets. An example histograms of differences between the LSTs derived by proposed approach and the ones from LSA SAF are presented at Fig 1a, 1b.

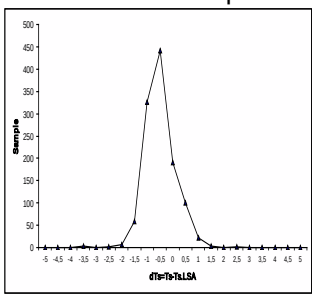

Figure 1a. **Histogram of differences T_S-$T_{S.LSA}$ for the first ROI, 02.06.2009.**

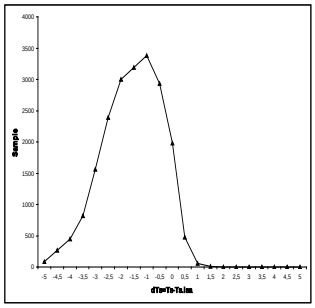

Figure 1b. **Histogram of differences T_S-$T_{S.LSA}$ for the second ROI, 02.06.2009.**

Along with this ROI selection the Ts retrieval experiments have been performed for the whole European region. The zenith angle range for this region is demonstrated at Fig.2.

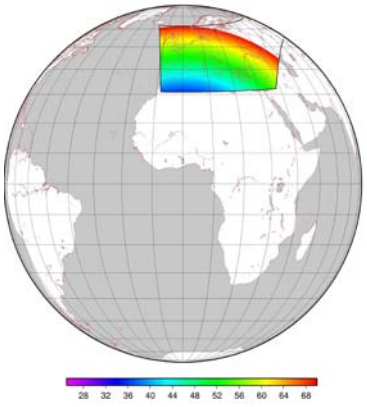

Figure 2. **Zenith angles for the European region.**

An example of both LSA SAF product and our LST estimates for the European region is shown at Fig.3a and Fig 3b. It appears that the temperature values on both figures are very close to each other for the covered areas. The amount of cloud-free pixels for the proposed approach is less than in LSA SAF due to the different cloud mask derivation procedure.

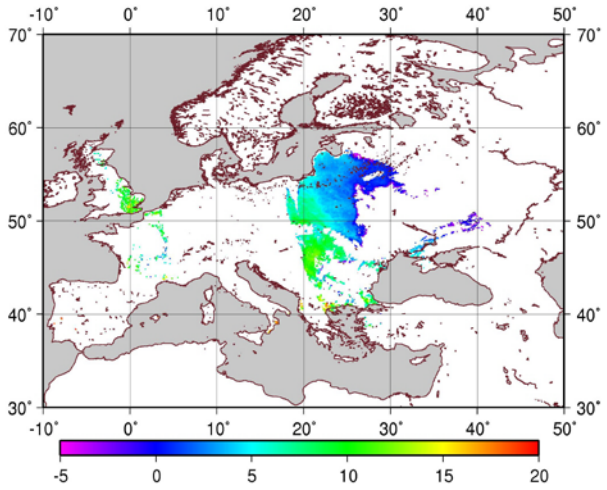

Figure 3a. **LST map derived with the proposed approach**

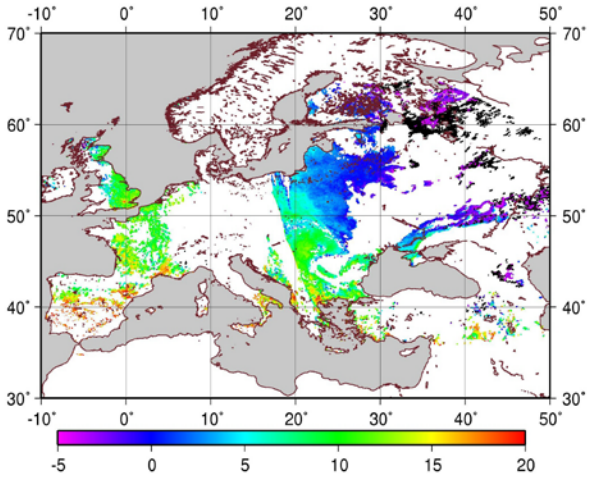

Figure 3b. **LST map from LSA SAF data**

The results of intercomparison with LSA SAF product for some dates in period from May to November 2009 are summarized in Table 1. Here Count means the sample size; Bias means averaged systematic discrepancy; RMSD – root-mean-square deviation between both data sets.

Date	Count	Bias	RMSD	RMSD with bias subtracted
02.11.2009	19 948	0.4157	0,9475	0,8514
07.09.2009	23 550	-2,2498	2,6224	1,6110
24.08.2009	18 450	-2,1104	2,4621	1,8603
13.07.2009	10 406	-0,4376	2,1695	2,1494
27.06.2009	3 839	-1,9171	2,5065	2,1506
02.06.2009	20 605	-1,5666	1,9312	1,5112
31.05.2009	17 941	-1,9000	2,2439	1,4611

Table 1. **Statistics of intercomparison between T_s estimates and LSA SAF product.**

It is clear from the table that subtracting of systematic bias significantly affects RMSD. The result of this operation is graphically presented at Fig.4

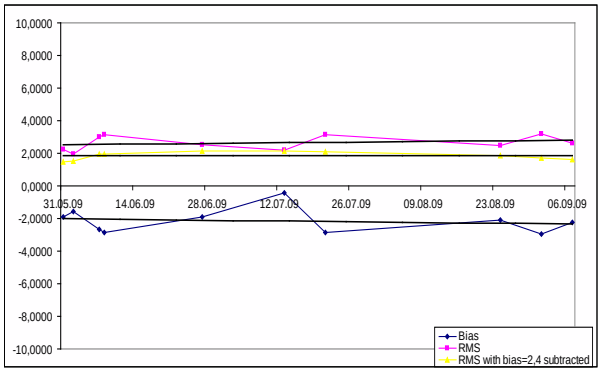

Figure 4. **Graphical representation of intercomparison statistics.**

CONCLUSIONS

1. A new method has been developed for LST derivation based on SEVIRI measurements in clear sky conditions. The method does not require predefined information about LSE in sounding points.

2. A cross-validation was performed with LSA SAF products disseminated via EUMETCast. It shows good level of correlation, which could be treated as indirect proof of method's efficiency.

3. Root-mean-square deviation between the above mentioned LST estimates is about 0.9-2.6K. It could be shifted down by subtracting a systematic biases.

Further works will include

- Comparisons of LST estimates with MODIS-based LSTs and in-situ data.
- Comparisons of LSE estimates to independent data
- Adaptation of developed methodology to MSU-GS data.

This research was partly funded within the RFBR projects №№07-05-13585; 07-05-01030.

REFERENCES

1. Becker, F. and Z.-L. Li, (990) Toward a local split-window method over land surface. Int. J. Remote Sens., vol. 11, N3, pp. 369-393.

2. Becker F, Z.-L. Li, (995) Surface temperature and emissivity at various scales: definition, measurement and related problems. Rem. Sens. Rev., v. 12, pp. 225-253.

3. Faysash, A. and E.A. Smith, (2000) Simultaneous Retrieval of Diurnal to Seasonal Surface Temperatures and Emissivities over SGP ARM-CART Site Using GOES Split Window - J. Appl. Meteor., vol. 39, pp. 971-982.

4. Labrot T., Lavanant L., White K. et al., (2006) AAPP Documentation. Scientific description - NWP SAF. Doc. NWP SAF-MF-UD-001, ver.6.0, 99p.

5. Product User Manual. Land Surface Temperature - SAF/LAND/IM/PUM_LST/2.1, 2008, 49p.

6. Saunders R.W., Matricardi M., Brunel P., (1999) An Improved Fast Radiative Transfer Model for Assimilation of Satellite Radiance Observations Q.J.R. Meteorol. Soc. v. 125, p.1407-1425.

7. Schmetz J., Pili P., Tjemkes S., D. Just, et al., (2002) An introduction to Meteosat Second Generation (MSG) Bull. Amer. Meteor. Soc., v. 83, pp. 977-992.

8. Snyder W.C., Wan Z., Zhang Y, and Y.-Z. Feng., (1998) Classification-based emissivity for land surface temperature measurement from space Int. J. Rem. Sens., vol. 19, N. 14, pp. 2753-2774.

9. Solovjev V.I., Uspensky S.A., (2009) Monitoring of land surface temperatures based on second generation geostationary meteorological satellites, Earth Studies from Space, №3, pp.17-25, (in Rassian).

10. Wan Z., J. Dozier., (1996) A generalised split-window algorithm for retrieving land surface temperature from space IEEE Trans. Geosci. Rem. Sens., vol. 34, N4, pp. 892-905.